Intensity correlations between the components of the resonance fluorescence triplet

C. A. Schrama,* G. Nienhuis,† H. A. Dijkerman, C. Steijsiger, and H. G. M. Heideman
Buys Ballotlaboratorium, Rijksuniversiteit Utrecht, Postbus 80 000, 3508 TA Utrecht, The Netherlands
(Received 6 November 1991)

We present a theoretical analysis of the intensity correlations between the spectral components of the resonance fluorescence triplet while allowing for detection time differences that are smaller than the inverse frequency width of the frequency filter. Explicit expressions are derived for the intensity correlation functions that are valid for all times. Furthermore, we present the results of measurements on these correlation functions for the $^1S_0 \leftrightarrow {}^1P_1$ resonance transition of natural barium. In general, the results confirm the theoretical predictions.

PACS number(s): 42.50.Dv, 32.80.−t

I. INTRODUCTION

The spectrum of resonance fluorescence of a two-state atom contains three well-separated spectral lines at sufficiently high intensity of the monochromatic driving field. This fluorescence triplet, which was predicted by Newstein [1] and Mollow [2], has been observed by a number of authors [3] and is sometimes referred to as the Mollow triplet. The three lines may be understood as resulting from spontaneous decay down a ladder of pairs of dressed states [4]. These states are energy eigenstates of the atom and the driving mode of the radiation field.

The same picture can explain the behavior of the correlation function between two successively detected photons originating from two spectral components [4]. Since the required spectral resolution imposes a limit on the possible time resolution, the theoretical description of this type of measurement is rather subtle. In particular, it is necessary to include the interferometer, used to separate the spectral components, explicitly in the theoretical description, as is common in the theory of time-dependent spectra [5]. A theoretical description of the time correlations between the spectral components of resonance fluorescence has been worked out for the special case of well-separated spectral lines, and for times larger than the inverse-frequency width of the interferometer [4,6,7]. The theoretical predictions have been verified experimentally in only one special case [8]. In this article we present a theoretical treatment of the correlation functions for times that are of the order of the filling time of the interferometer and we report experiments on the intensity correlations between all possible combinations of the spectral components of the fluorescence triplet.

The simple interpretation of the spectrally resolved correlation functions in terms of transitions between the modified energy levels is justified for correlation times that are large compared with the filling time of the interferometer. This picture is slightly modified if times are considered that are of the order of the filling time. In the latter case the order of detection is not necessarily the same as the order of emission. For an observed detection order, interference can arise between opposite emission orders.

In the following we give a summary of the derivation of the long-time behavior of the two-time intensity correlation functions for frequency-filtered fields. The short-time behavior is derived for the case that the fluorescence field is emitted by a two-state atom in a monochromatic field. We report an experimental study of the various intensity correlation functions.

II. INTENSITY CORRELATIONS AND SPECTRAL RESOLUTION

The intensity correlation function $I_2(t_1,t_2)$ of a radiation field is measured as the probability density for detecting a photon at time t_1 and another at time t_2. For a quantum field, the ordering of the field operators in a transition amplitude is essential. When we denote the absorptive positive-frequency part of the electric field as $E^+(t)$, the quantum-mechanical expression for the correlation function for $t_2-t_1>0$ is [9]

$$I_2(t_1,t_2)=(2\epsilon_0 c)^2\langle E^-(t_1)E^-(t_2)E^+(t_2)E^+(t_1)\rangle \ . \quad (1)$$

This expression may be viewed as the averaged square of the amplitude for two successive absorptions at time t_1 and t_2. If the radiation field is emitted by an atomic transition from an excited state $|e\rangle$ to a ground state $|g\rangle$, then the Heisenberg operators E^+ (E^-) for the field are proportional to the lowering part S^- (raising part S^+) of the atomic dipole transition, so that we may write [10]

$$E^+(t)\sim S^-(t) \ , \quad E^-(t)\sim S^+(t) \quad (2)$$

with

$$S^-=|g\rangle\langle e| \ , \quad S^+=|e\rangle\langle g| \ . \quad (3)$$

For a single atom we obtain for the intensity correlation function the expression

$$I_2(t_1,t_2)=(\eta A)^2\langle S^+(t_1)S^+(t_2)S^-(t_2)S^-(t_1)\rangle \ , \quad (4)$$

with A the spontaneous-decay rate and η the detection probability of an emitted photon.

We consider the case of a two-state atom in a monochromatic radiation field with frequency ω_l, so that the detected radiation is resonance fluorescence. We use a classical description of the exciting field, and we adopt the dipole and the rotating-wave approximation. In the rotating frame the evolution of the atomic density matrix σ is described by the evolution equation

$$\frac{d\sigma}{dt}=-(iL+\Gamma)\sigma \ . \tag{5}$$

The operator Γ, which describes spontaneous decay, is given by [11]

$$\Gamma\sigma=\tfrac{1}{2}A(S^+S^-\sigma+\sigma S^+S^--2S^-\sigma S^+) \ . \tag{6}$$

The operator L indicates the commutator with an effective Hamiltonian

$$-iL\sigma=-i[H,\sigma]/\hbar \ , \tag{7}$$

where

$$H=-\hbar(\Delta S_z+\Omega S_x) \ . \tag{8}$$

The Pauli matrices have the standard form

$$\begin{aligned} S_x&=\tfrac{1}{2}(|e\rangle\langle g|+|g\rangle\langle e|) \ , \\ S_y&=\frac{1}{2i}(|e\rangle\langle g|-|g\rangle\langle e|) \ , \\ S_z&=\tfrac{1}{2}(|e\rangle\langle e|-|g\rangle\langle g|) \ , \end{aligned} \tag{9}$$

$\Delta=\omega_l-\omega_0$ is the detuning from resonance, and Ω is the Rabi frequency.

In the steady state the intensity correlation function (4) depends only on the time difference $t_2-t_1=t$ and we may write

$$\begin{aligned} I_2(t_1,t_1+t)&=(\eta A)^2\mathrm{Tr}S^-[e^{-(iL+\Gamma)t}(S^-\bar{\sigma}S^+)]S^+ \\ &\equiv I_1 f(t) \ . \end{aligned} \tag{10}$$

Here we introduced $\bar{\sigma}$ as the normalized steady-state solution of (5). Furthermore,

$$I_1=\eta A\ \mathrm{Tr}S^-\bar{\sigma}S^+=\eta A\langle e|\bar{\sigma}|e\rangle \tag{11}$$

is the steady-state photon detection rate, and

$$f(t)=\eta A\ \mathrm{Tr}|e\rangle\langle e|(e^{-(iL+\Gamma)t}|g\rangle\langle g|) \tag{12}$$

is the conditional detection rate at time t after a previous detection at time zero. Explicit expressions for $f(t)$ are given in the literature [12]. From (12) it is obvious that $f(0)=0$, which indicates that after a photon emission the atom cannot immediately emit a subsequent photon [10,13]. This phenomenon is called antibunching.

These standard results apply in the situation that the instants of photon emission are determined. This can only be the case if the photons are detected without spectral resolution. For the description of our experiments we need a theoretical analysis of correlated detections of photons with a well-determined frequency. In practice this means that the two photomultipliers which detect the photons are viewing the radiation field exiting an interferometer. This implies that the fields in (1) should be replaced by the filtered fields $\bar{E}^{\pm}$, which are to a good approximation related to the emitted field by the relation [5]

$$\bar{E}^+_\alpha(t)=\int_0^\infty d\tau\, e^{-i\omega_\alpha\tau}\gamma e^{-\gamma\tau}E^+(t-\tau) \ , \tag{13}$$

with γ the bandwidth of the interferometer, and ω_α its frequency setting. The normalization of (13) is chosen in such a way that in the case of a monochromatic field of frequency ω_α, the filtered field is identical to the incident field. Factors resulting from filter transmittivities can simply be absorbed in the overall detection efficiency η. For classical radiation fields, the correlation function $\bar{I}_2(\alpha t_1;\beta t_2)$ for observation of a photon from interferometer α at time t_1 and a photon from interferometer β at time t_2 is obtained by substituting $\bar{E}^{\pm}_\alpha(t_1)$ for $E^{\pm}(t_1)$ and $\bar{E}^{\pm}_\beta(t_2)$ for $E^{\pm}(t_2)$ into (1). The result is a fourfold integral over a four-point correlation function.

For the present case of resonance fluorescence the field is essentially quantum mechanical, and the situation is more delicate. As has been demonstrated by various authors [14,15], for a quantum field where the time ordering of the field operators is essential, we have to reorder the operators $E^{\pm}$ so that the earlier absorption operators E^+ are moved to the right, and the earlier emission operators are moved to the left. After expressing the field operators $E^{\pm}$ in terms of the atomic operators $S^{\mp}$, as in (2), we arrive at the explicit formal expression for the correlation function for spectrally resolved photons ($t_2>t_1$)

$$\begin{aligned} \bar{I}_2(\alpha t_1;\beta t_2)=(\eta A)^2\int_0^\infty & d\tau_1 d\tau_2 d\tau_1' d\tau_2' \gamma^4 e^{-\gamma(\tau_1+\tau_2+\tau_1'+\tau_2')} e^{-i\omega_\alpha(\tau_1-\tau_1')} e^{-i\omega_\beta(\tau_2-\tau_2')} \\ &\times[\Theta(t_2-\tau_2-t_1+\tau_1)\Theta(t_2-\tau_2'-t_1+\tau_1')\langle S^+(t_1-\tau_1')S^+(t_2-\tau_2')S^-(t_2-\tau_2)S^-(t_1-\tau_1)\rangle \\ &+\Theta(t_2-\tau_2-t_1+\tau_1)\Theta(t_1-\tau_1'-t_2+\tau_2')\langle S^+(t_2-\tau_2')S^+(t_1-\tau_1')S^-(t_2-\tau_2)S^-(t_1-\tau_1)\rangle \\ &+\Theta(t_1-\tau_1-t_2+\tau_2)\Theta(t_2-\tau_2'-t_1+\tau_1')\langle S^+(t_1-\tau_1')S^+(t_2-\tau_2')S^-(t_1-\tau_1)S^-(t_2-\tau_2)\rangle \\ &+\Theta(t_1-\tau_1-t_2+\tau_2)\Theta(t_1-\tau_1'-t_2+\tau_2') \\ &\times\langle S^+(t_2-\tau_2')S^+(t_1-\tau_1')S^-(t_1-\tau_1)S^-(t_2-\tau_2)\rangle] \ , \end{aligned} \tag{14}$$

where Θ is the Heaviside step function. One notices that the spectral resolution corresponding to the bandwidth γ of the interferometers implies an indeterminacy in the instants of emission, even though the detection times are known. The evaluation of (14) requires the calculation of four-time correlation functions of the atomic dipole, which in general is a very tedious task, and the resulting general expression is not illuminating in its complexity. The physical picture of the correlation process becomes much clearer in the case that the fluorescence spectrum separates into different spectral lines. Then also the explicit evaluation of (14) becomes much simpler, as we shall demonstrate in the next section.

III. SEPARATE FLUORESCENCE LINES

It is well known that the spectrum of resonance fluorescence of a two-state atom separates into three distinct spectral lines at high intensity of the driving field or at large detuning from resonance [2]. A simple physical picture of the origin of these lines arises if we diagonalize the effective Hamiltonian (8). The eigenstates are related to the atomic states $|e\rangle$ and $|g\rangle$ by a simple rotation, according to

$$|1\rangle = c|g\rangle - s|e\rangle, \quad |2\rangle = s|g\rangle + c|e\rangle \tag{15}$$

with

$$c = \left[\frac{\Omega'+\Delta}{2\Omega'}\right]^{1/2}, \quad s = \left[\frac{\Omega'-\Delta}{2\Omega'}\right]^{1/2}, \tag{16}$$

and

$$\Omega' = (\Omega^2+\Delta^2)^{1/2}, \tag{17}$$

determining the eigenvalues $E_1 = \frac{1}{2}\hbar\Omega'$, $E_2 = -\frac{1}{2}\hbar\Omega'$. The states (15) are the classical versions [16] of the dressed-atom eigenstates [17]. Fluorescent emission arises as spontaneous decay down a ladder of pairs of states (15), where the subsequent pairs are separated by one photon energy $\hbar\omega_l$ of the radiation field. Transitions $|1\rangle \rightarrow |1\rangle$ and $|2\rangle \rightarrow |2\rangle$ give rise to emission at frequency ω_l, and two sidebands at $\omega_l \pm \Omega'$ arise from the transition $|1\rangle \rightarrow |2\rangle$ and $|2\rangle \rightarrow |1\rangle$. These transitions are illustrated in Fig. 1. The spectrum consists of three separate lines when the line separation Ω' is considerably larger than their width, which is of the order of the spontaneous decay rate A. The central line at frequency ω_l is the Rayleigh line (R). For $\Delta > 0$, the low-frequency sideband is nearest to the atomic resonance, and it is called the fluorescence line (F). The high-frequency sideband can be understood to arise from a three-photon excitation [17], and it is termed the three-photon line (T).

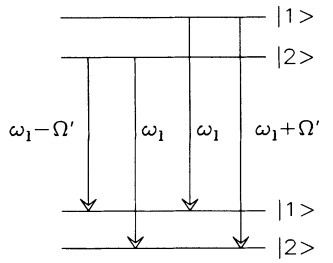

FIG. 1. The lines in the fluorescence spectrum arise from radiative transitions between the dressed states $|1\rangle$ and $|2\rangle$.

In the limit of well-separated lines $\Omega' \gg A$, when the frequency separation between the dressed states $|1\rangle$ and $|2\rangle$ is large compared with their width, the evolution equation (5) for the atomic density matrix can be approximated by neglecting the coupling between the dressed-state coherences and populations. The diagonal part

$$\sigma_d = |1\rangle n_1 \langle 1| + |2\rangle n_2 \langle 2| \tag{18}$$

then obeys a closed evolution equation

$$\frac{d\sigma_d}{dt} = -\Gamma_d \sigma_d, \tag{19}$$

where Γ_d is the projection of the spontaneous-decay operator Γ on the subspace of diagonal matrices. We separate the atomic decay operator S^- into a sum of decay operators between dressed states according to

$$S^- = S_F^- + S_T^- + S_R^-, \tag{20}$$

with

$$\begin{aligned} S_F^- &= c^2|1\rangle\langle 2|, \\ S_T^- &= -s^2|2\rangle\langle 1|, \\ S_R^- &= cs(|2\rangle\langle 2| - |1\rangle\langle 1|). \end{aligned} \tag{21}$$

Then we obtain for the approximate evolution of σ_d the equation

$$-\Gamma_d\sigma_d = -\tfrac{1}{2}A \sum_{\alpha=F,T} (S_\alpha^+ S_\alpha^- \sigma_d + \sigma_d S_\alpha^+ S_\alpha^- - 2S_\alpha^- \sigma_d S_\alpha^+). \tag{22}$$

Note that the contribution of $S_R^\pm$ may be ignored in (22) since $S_R^+ = S_R^-$ commutes with σ_d. The physical significance of this fact is that emission of a photon in the Rayleigh line does not modify the dressed-state populations.

The explicit form of the evolution equation for the dressed-state populations is

$$\frac{dn_1}{dt} = -As^4 n_1 + Ac^4 n_2 = -\frac{dn_2}{dt}, \tag{23}$$

with the obvious steady-state solutions

$$\bar{n}_1 = \frac{c^4}{c^4+s^4}, \quad \bar{n}_2 = \frac{s^4}{c^4+s^4}. \tag{24}$$

The total fluorescence intensity (11) can be expressed as the sum of the three separate line intensities

$$\bar{I}_\alpha = \eta A \, \mathrm{Tr} S_\alpha^- \bar{\sigma}_d S_\alpha^+ \tag{25}$$

for $\alpha = F, T, R$. This gives

$$\bar{I}_F = \bar{I}_T = \eta A \frac{c^4 s^4}{c^4+s^4}, \quad \bar{I}_R = \eta A c^2 s^2. \tag{26}$$

A. Long-time behavior

We now turn to the spectrally resolved intensity correlation function (14) in the limit of separated lines. When the frequency settings ω_α and ω_β are tuned to the frequencies of components of the fluorescence triplet, the picture of fluorescence as arising from spontaneous transitions between dressed states leads to simple generalizations of (10)

$$\bar{I}_2(\alpha\beta;t)=(\eta A)^2\mathrm{Tr}S_\beta^-[e^{-\Gamma_d t}(S_\alpha^-\bar{\sigma}_d S_\alpha^+)]S_\beta^+ \quad (27)$$

for $\alpha,\beta=F,T,R$, where we abbreviate $\bar{I}_2(\alpha t_1;\beta t_1+t)=\bar{I}_2(\alpha\beta;t)$. Furthermore, we introduce the normalized correlation function $g_2(\alpha\beta;t)=\bar{I}_2(\alpha\beta;t)/\bar{I}_\alpha\bar{I}\beta$. In the structure of (27) one recognizes the emission of a photon in the line α by the steady-state atom, a subsequent evolution during the time t, and finally the emission of a photon in the line β. Special cases of (27) have been derived by various authors [4,6,7,18]. The correlation functions for two photons from a single sideband are given by

$$g_2(FF;t)=g_2(TT;t)=1-e^{-A(c^4+s^4)t}\ . \quad (28)$$

These functions display antibunching behavior, which simply results from the fact that after the first emission the atom has no population in the dressed state from which the second emission is possible. Conversely, the correlation functions between opposite sidebands have the explicit expressions

$$g_2(TF;t)=1+\frac{c^4}{s^4}e^{-A(c^4+s^4)t}\ , \quad (29a)$$

$$g_2(FT;t)=1+\frac{s^4}{c^4}e^{-A(c^4+s^4)t}\ . \quad (29b)$$

These functions display bunching behavior, since after the first emission the atom ends up in the initial state for transition corresponding to the second emission [4,18]. Furthermore, for $\Delta\gg\Omega$ for $c^4/s^4\gg1$, there is a strong time asymmetry in the emission order of F and T photons. They tend to arrive in pairs, with the T photon preceding the F photon [4,6]. This has been observed in an experiment on Sr atoms [8]. Finally, if we apply (27) to correlations functions involving a photon from the central Rayleigh line, they are found to be independent of time, so that [6,7]

$$g_2(R\alpha;t)=g_2(\alpha R;t)=1\ . \quad (30)$$

This reflects that emission of a Rayleigh photon does not modify the density matrix σ_d, and that the emission rate of Rayleigh photons is independent of the dressed-state populations.

The validity of these simple explicit results (27)–(30) depends on a number of restrictive assumptions. The condition already emphasized elsewhere [4,6] is

$$\Omega'\gg\gamma\gg A\ . \quad (31)$$

The first inequality $\Omega'\gg\gamma$ implies that the bandwidth of the *spectrometers* is sufficiently narrow to distinguish the separate lines. Conversely, this also means that the rapid oscillations of the dressed-state coherences at the precession frequency Ω' are smeared out by the limited time resolution γ^{-1}. The second inequality $\gamma\gg A$ requires that each photon from a spectral component has equal probability of being detected, so that no deformation of the spectral line arises. As viewed in the time domain, this means that the uncertainty in the emission time is small on the time scale of the evolution through spontaneous decay. In the language of (14) these two assumptions (31) imply that the dressed-state coherences, which oscillate at the frequency Ω', yield negligible contributions, and that the time differences $\tau_1-\tau_1'$ and $\tau_2-\tau_2'$ are negligible on the remaining slow time scale.

Here we wish to emphasize that the conditions (31) are not sufficient for the validity of (27)–(30). An additional condition [7] is the requirement that

$$t\gg\gamma^{-1}\ . \quad (32)$$

This condition ensures that the order of the detection times t_1 and $t_2=t_1+t$ is the same as the order of the emission times $t_1-\tau_1$ and $t_2-\tau_2$ (or $t_1-\tau_1'$ and $t_2-\tau_2'$). Then only the first term in (14) contributes, and there is no uncertainty in the order of emission for a given order of detection.

B. Short-time behavior

We now proceed to generalize (27) for the case that the condition (32) is no longer valid. However, we still assume the validity of (31). First we consider the case that

$$t\ll A^{-1}\ . \quad (33)$$

Then all the time arguments in the integrand of (14) may be assumed to be close together compared with the slow evolution time A^{-1}. On the other hand, when ω_α and ω_β in (14) are taken at the frequency position of components of the triplet, the rapid oscillations cancel only if we substitute for the operators $S^\pm$ the corresponding transition operators $S_\alpha^\pm$ and $S_\beta^\pm$. The resulting expression for the intensity correlation function (14) is then for $t\ll A^{-1}$

$$\bar{I}_2(\alpha\beta;t)=(\eta A)^2\int_0^\infty d\tau_1 d\tau_2 d\tau_1' d\tau_2'\gamma^4 e^{-\gamma(\tau_1+\tau_2+\tau_1'+\tau_2')}\mathrm{Tr}\bar{\sigma}_d[\Theta(t-\tau_2'+\tau_1')S_\alpha^+S_\beta^+ +\Theta(-t+\tau_2'-\tau_1')S_\beta^+S_\alpha^+]$$
$$\times[\Theta(t-\tau_2+\tau_1)S_\beta^-S_\alpha^- +\Theta(-t+\tau_2-\tau_1)S_\alpha^-S_\beta^-]\ . \quad (34)$$

Note that we only need expectation values of products of operators at a single time instant. In the first term, the α photon is emitted first, and in the last term the order of emission is reversed. The second and third term constitute interference between opposite time orders.

The integral (34) can be evaluated directly and we find for $t\ll A^{-1}$

$$\bar{I}_2(\alpha\beta;t)=(\eta A)^2[(1-\tfrac{1}{2}e^{-\gamma t})^2\mathrm{Tr}\bar{\sigma}_d S_\alpha^+ S_\beta^+ S_\beta^- S_\alpha^- + \tfrac{1}{2}e^{-\gamma t}(1-\tfrac{1}{2}e^{-\gamma t})\mathrm{Tr}\bar{\sigma}_d(S_\alpha^+ S_\beta^+ S_\alpha^- S_\beta^- + S_\beta^+ S_\alpha^+ S_\beta^- S_\alpha^-)+(\tfrac{1}{2}e^{-\gamma t})^2\mathrm{Tr}\bar{\sigma}_d S_\beta^+ S_\alpha^+ S_\alpha^- S_\beta^-] \ . \quad (35)$$

Obviously, the correlation function between two photons from the same line ($\alpha=\beta$) is not affected by the uncertainty in time orderings, and then (35) is simply equal to the short-time limit of (27). We conclude that (28) remains valid also when condition (32) is not met. Likewise, for the correlation function between two Rayleigh photons the result

$$g_2(RR;t)=1 \quad (36)$$

remains unchanged.

On the other hand, for $\alpha\neq\beta$ the expectation values in (35) are not all identical, and effects of the time ordering arise for $t\lesssim\gamma^{-1}$. First we consider the case that $\alpha=F$, $\beta=R$. From Fig. 1 we notice that emission of an F photon and an R photon can occur as a direct cascade $|2\rangle\rightarrow|1\rangle\rightarrow|1\rangle$, or as a cascade $|2\rangle\rightarrow|2\rangle\rightarrow|1\rangle$. In the former possibility the emission of the F photon is the first one, and in the latter case the R photon is emitted first. Then two different cascades constitute a transition from the same initial to the same final state of the dressed atom and the fluorescence field. On the other hand, the amplitudes for these two processes are each other's opposite, since (21) shows that

$$S_F^- S_R^- = c^3 s|1\rangle\langle 2| = -S_R^- S_F^- \ . \quad (37)$$

Therefore, for $t=0$, where both time orderings contribute equally, the correlation function must disappear. In general, we obtain from (35) the explicit result

$$g_2(FR;t)=g_2(RF;t)=(1-e^{-\gamma t})^2 \ , \quad (38)$$

which is valid for all values of $t>0$. For $t\gg\gamma^{-1}$, the long-time result (30) for $\alpha=F$ is recovered. The dip at $t=0$ is due to destructive interference between the two time orderings. It is important to notice that this interference arises due to the uncertainty in the instants of emission for observed detection times. This uncertainty reflects the finite filling time of the interferometers, which are normally located at a macroscopic distance from the emitting atom. The interference dip gets broader when the bandwidth is decreased. In Fig. 2 Eq. (38) is plotted (curve *b*).

The same arguments hold for correlation between a T photon and an R photon. The result which is valid for all values of $t>0$ is

$$g_2(TR;t)=g_2(RT;t)=(1-e^{-\gamma t})^2 \ . \quad (39)$$

Finally we consider the cases $\alpha=F$, $\beta=T$, and $\alpha=T$, $\beta=F$. It is easy to check that only the first and the last term in (35) contribute, while the interference terms vanish. If we combine the long-time expressions (29) with the explicit result (35) for $t\ll A^{-1}$ we arrive, for this choice of α and β, at an expression valid for all values of $t>0$ of the form

$$g_2(TF;t)=\frac{c^4}{s^4}(e^{-A(c^4+s^4)t}-1)+\left[1+\frac{c^4}{s^4}\right](1-\tfrac{1}{2}e^{-\gamma t})^2 + \left[1+\frac{s^4}{c^4}\right](\tfrac{1}{2}e^{-\gamma t})^2 \quad (40a)$$

and

$$g_2(FT;t)=\frac{s^4}{c^4}(e^{-A(c^4+s^4)t}-1)+\left[1+\frac{s^4}{c^4}\right](1-\tfrac{1}{2}e^{-\gamma t})^2 + \left[1+\frac{c^4}{s^4}\right](\tfrac{1}{2}e^{-\gamma t})^2 \ . \quad (40b)$$

Equations (40) combined give the full correlation function for detection of a T photon and an F photon, both for positive and negative time differences (see Fig. 2, curve *a*). For $t\gg\gamma^{-1}$, the long-time behavior of Eqs. (29) is recovered, while in the region where $t\ll A^{-1}$ only the contribution of (35) survives. For $t=0$, (40a) and (40b) give the same value, so that the correlation between a T and an F photon varies continuously at equal detection times. For $\Delta\gg\Omega'$ or $c^4/s^4\gg1$, the two results (40a) and (40b) display in the region $t\simeq0$ a rapid transition over a time range γ^{-1} between the strongly different long-time functions (29a) and (29b). In the resonance case that $\Delta=0$, we have $c^4=s^4=\frac{1}{4}$ and the physical difference between an F transition and a T transition vanishes. Then (40a) and (40b) become identical, and the FT correlation function is even in the detection time difference. Note that Eqs. (40) predict a dip of width γ^{-1} at $t=0$, which exactly compensates the bunching behavior of Eqs. (29), so that for the resonant case we have the equal-time result

$$g_2(TF;0)=1 \ . \quad (41)$$

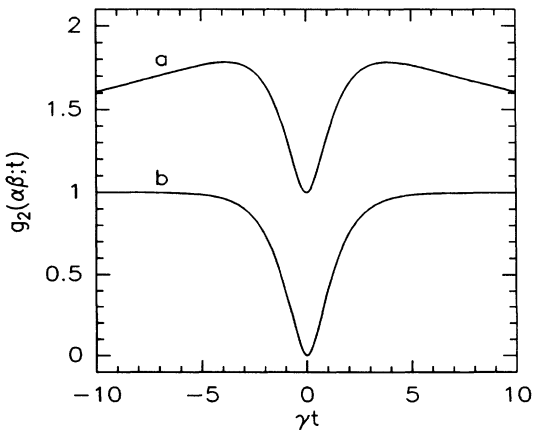

FIG. 2. $g_2(\alpha\beta;t)$ vs γt for $\Omega=100A$, $\Delta=0$, and $\gamma=10A$; *a*, $\alpha\beta=FT$; *b*, $\alpha\beta=FR$.

The origin of this dip lies in the fact that the interference terms in (35) vanish for the FT correlation function. For time differences of the order of γ^{-1} or less, the amplitude for detection of an F and a T photon is a weighted sum of the amplitudes for the two emission orders. Since in the detection probability the contribution from the cross terms are missing, this leads to a decrease of the correlation function near zero time difference. For $t=0$, both emission orders have equal weight, and the value of g_2 is half the zero-time limit of the bunching long-time functions (29).

IV. EXPERIMENTAL SETUP

Although in correlation experiments sodium is often used [12,19], we have used the $^1S_0 \leftrightarrow {}^1P_1$ transition of barium at $\lambda=553.5$ nm. The influence of the isotopes and the metastable D states can be neglected if the metal is excited on the low-frequency side of the ^{138}Ba resonance transition and if the average time during which the atom is observed is too short to branch into the D states substantially [20,21].

A schematic overview of the experimental arrangement is given in Fig. 3. The experiments are performed in a dilute atomic beam of natural barium. In a high-vacuum chamber the barium beam is produced in a cylindrical tantalum oven. The atoms leave the oven through a circular aperture, $\phi=2.1$ mm. A pinhole having a diameter of 0.1 mm collimates the beam to a diameter of 0.25 mm and a divergence of $\vartheta=3$ mrad (full width). The pinhole is placed 5×10^{-2} m from the interaction region. The distance between the microscope objectives and the oven is 0.8 m.

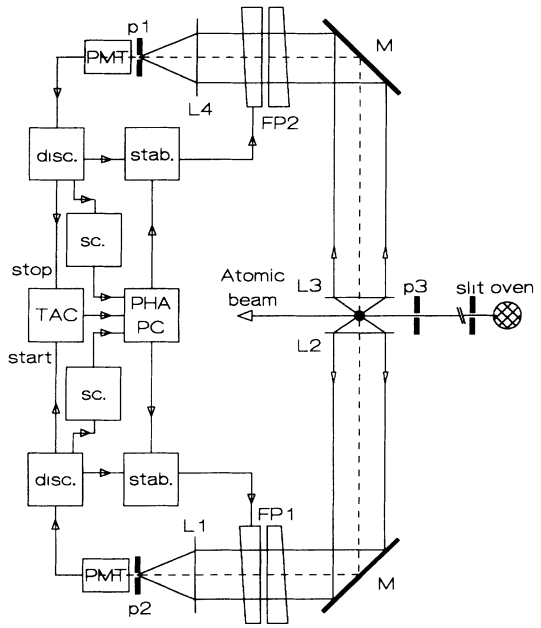

FIG. 3. Experimental setup for photon correlation experiments with spectral resolution. The diameter of the oven aperture is 2.1 mm. p1,p2: pinholes $\phi=0.5$ mm; p3: pinhole $\phi=0.1$ mm; L2, L3: microscope objectives L1, L4: achromatic lenses $f=254$ mm; PMT: photomultiplier; disc.: discriminator; sc: singles counter; TAC: time-to-amplitude converter; PHA: pulse-height analyzer; PC: personal computer; M: mirror; stab.: stabilization unit; FP1,FP2: Fabry-Pérot interferometers. The dot between the microscope objectives indicates the position of the laser beam.

A single-mode laser beam, which is linearly polarized, is focused on the atomic beam with an achromatic lens of 160 mm focal length. This beam is obtained from a system where an Ar^+ laser pumps a frequency stabilized single-mode cw dye laser (Spectra-Physics, model 380D) operating on Rhodamine-110. Typical output power is 800 mW. On resonance the long-term frequency drift is checked for by monitoring the singles count rates in the detection channels. The laser frequency is readjusted manually whenever necessary. For experiments off resonance the laser is locked to the lower-frequency flank of the absorption profile of a heat-pipe cell filled with natural Ba [22]. With this additional stabilization the residual long-time variation in the laser frequency is less than 10 MHz. This is mainly due to fluctuations in the vapor pressure caused by variations in the temperature of the cell.

Stray light from the laser is reduced by a small aperture just above the interaction region. Two microscope objectives, one on each side of the interaction region, the focus from which coincides with the interaction region, collect the fluorescence and produce a parallel beam of light. In each detection channel an achromatic lens focuses this beam on a pinhole. In both detection channels a Fabry-Pérot interferometer (Burleigh RC-110 and RC-150) is placed outside the vacuum chamber, between the microscope objective and the achromatic lens. The fluorescence photons are detected by two photomultipliers whose output pulses are fed into constant-fraction discriminators. A time-to-amplitude converter (TAC) measures the time differences between the photon pulses and sends its output to a 1024 channel pulse-height analyzer (PHA) which is part of a personal computer. Singles rates from each photomultiplier are measured by two rate meters.

The time resolution of the electronic detection system was measured by having both photomultipliers look at a scattering center which is irradiated by a pulsed Ar^+ laser (120 ps pulse width). By measuring the cross correlation between the two photomultipliers the time resolution of the combined system was found to be 3.1 ns.

Inside the interaction volume V, where the Ba beam crosses the laser beam and from which the fluorescence is collected, the number of atoms fluctuates around a mean value $\langle N \rangle$. The rate of true coincidences (two photons emitted by one and the same atom) scales with $\langle N \rangle$. The background, due to the accidental coincidences (two photons emitted by two different atoms), scales with $\langle N \rangle^2$. Hence the ratio of the number of true coincidences to the number of accidental coincidences decreases as $\langle N \rangle$ increases.

Kimble, Dagenais, and Mandel [23] derived an expression for the mean number of counts, $\langle n(t) \rangle$, in a channel of the PHA for experiments without spectral resolution. If the photomultipliers measure only the intensity from a

single component of the fluorescence triplet then $\langle n(t)\rangle$ takes the form

$$\langle n(t)\rangle \propto \langle N\rangle^2 \bar{I}_2(\alpha\beta;\infty)+\langle N\rangle \xi(t)\bar{I}_2(\alpha\beta;t)\ , \quad (42)$$

where $\xi(t)$ describes the effect of the transit of the atoms through the observation volume. To include effects of dark currents and the actual shape of the transmission function of the Fabry-Pérot extra terms must be added to (42).

Equation (42) shows that in a beam experiment there will always be a background term resulting from accidental coincidences. Furthermore, the correlation function $\bar{I}_2(\alpha\beta;t)$ is multiplied by a time-dependent factor $\xi(t)$ which drops to zero as $t\to\infty$. This can be understood by noting that it is only for a limited time that the emitting atom is in the field of view.

The transit function $\xi(t)$ as derived by Kimble, Dagenais, and Mandel [23] holds for two identical and perfectly coinciding observation volumes. We will consider two partially overlapping observation volumes, V_a and V_b, and derive a general expression for $\xi(t)$. It will be assumed that both volumes have the same rectangular shape and that an atom first enters V_a and then V_b, where V_a is seen by the start photomultiplier and V_b is seen by the stop photomultiplier. In both volumes the atom can be observed over a length l. The length over which the atom can be seen by both photomultipliers is $l'\le l$. We call $\xi'(t,v)$ the function that describes the probability of finding an atom with a velocity v in the stop region at t, given it was in the start region at $t=0$. This conditional probability is given by

$$\xi'(t,v)=\begin{cases}1-|1-q-vt/l| & \text{for } |1-q-vt/l|\le 1\\ 0 & \text{for } |1-q-vt/l|>1\ ,\end{cases} \quad (43)$$

with $q=l'/l$ (see Fig. 4). Since the experiments are performed in a thermal atomic beam $\xi'(t,v)$ has to be integrated over the velocity density distribution $P(v)=2(v^3/v_0^4)\exp(-v^2/v_0^2)$ with $v_0=\sqrt{2kT/m}$, T the oven temperature and m the mass of the atom. The resulting transit function is found to be

$$\xi(t)=\begin{cases}2\int_0^{-q\tau_0/t} dx\left[q+\dfrac{xt}{\tau_0}\right]x^3e^{-x^2} & \text{for } t\le 0\\ 2\int_0^{(1-q)\tau_0/t} dx\left[q+\dfrac{xt}{\tau_0}\right]x^3e^{-x^2}+2\int_{(1-q)\tau_0/t}^{(2-q)\tau_0/t} dx\left[2-q-\dfrac{xt}{\tau_0}\right]x^3e^{-x^2} & \text{for } t\ge 0\ ,\end{cases} \quad (44)$$

where $\tau_0=l/v_0$. For perfectly overlapping volumes ($q=1$) this general expression reduces to

$$\xi(t)=2\int_0^{\tau_0/|t|} dx\left[1-\frac{x|t|}{\tau_0}\right]x^3e^{-x^2}\ , \quad (45)$$

as derived by Kimble, Dagenais, and Mandel [23].

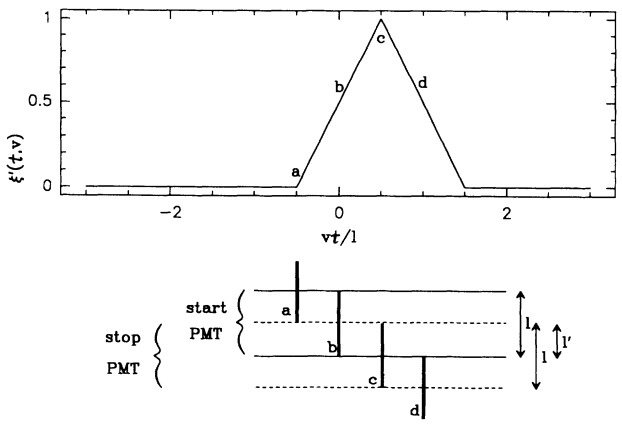

FIG. 4. $\xi'(t,v)$ for $q=\frac{1}{2}$. The vertical bars in the lower part of the figure indicate the range of possible positions at four different times of finding the atom along its path through the observation volumes, given it was in the start region at $t=0$. In the upper part the corresponding conditional probabilities are given of finding the atom in the stop region.

When an interferometer is tuned to one of the components of the fluorescence triplet a small amount of light of the other components will be transmitted. The transmission factor for these other components will be denoted as ζ_i with $i=a,b$.

In an experiment in which the interferometers are tuned to opposite sidebands the unwanted Rayleigh photons in the filtered fluorescence signal affect the spectra in two ways: (i) as an uncorrelated part contributing to the background term and (ii) as a correlated part contributing to the signal term. We denote by $\mathcal{R}_i$ the number of R photons in the filtered fluorescence field and by R_i the number of true F or T photons. The ratio of Rayleigh photons to the number of true sideband photons in the filtered fluorescence field is then given by

$$\frac{\mathcal{R}_i}{R_i}=\zeta_i\left[2+\frac{4\Delta^2}{\Omega^2}\right]\ . \quad (46)$$

Since we are only interested in correlations between sideband photons this ratio should be much smaller than one. For $\Delta\gg\Omega$ (large detuning) situations can occur where the fluorescence detected by the photomultipliers mainly consists of Rayleigh photons: $\mathcal{R}_i/R_i\gg 1$. Aspect *et al.* [8] have shown that in this situation it is still possible to measure correlations between the sideband photons provided that

$$\langle N\rangle\zeta_a\zeta_b\lesssim 1\ . \quad (47)$$

For all the other combination of lines in the fluores-

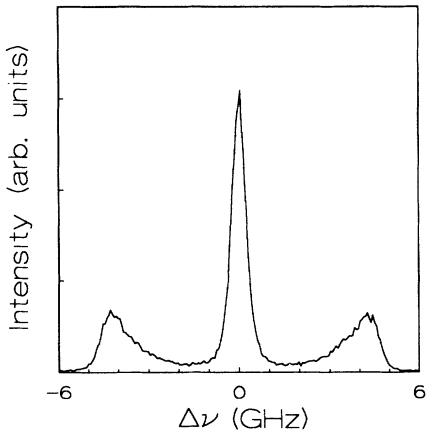

FIG. 5. Inhomogeneously broadened fluorescence spectrum on resonance. The inhomogeneous broadening is caused by the spatial profile of the laser beam.

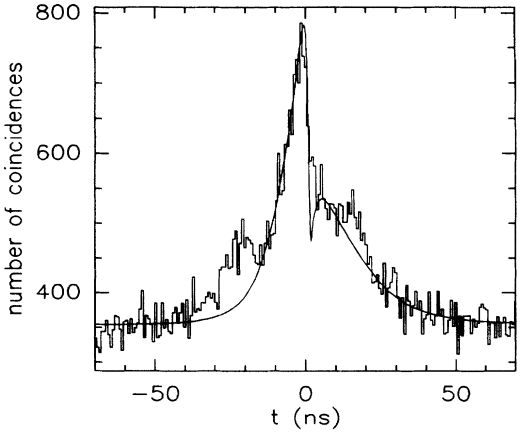

FIG. 7. The same as Fig. 6. $\Delta=-1.4(2)$ GHz and $\Omega=4.3(2)$ GHz.

cence triplet it can be easily shown from a similar treatment that the average number of atoms in the interaction volume should always be close to or less than one.

V. RESULTS AND DISCUSSION

The parameters c and s, (16), which determine the shapes of the correlation functions depend only on Δ/Ω. We have done experiments in which Δ was varied, while keeping Ω as large as possible, to ensure sufficient separation of the triplet components on resonance.

In Fig. 5 an example is given of the fluorescence triplet as recorded by one of the Fabry-Pérot interferometers. The fluorescence triplet is inhomogeneously broadened, which is caused by inhomogeneities in the laser intensity over the interaction volume. By tuning the Fabry-Pérot device to the maximum of a sideband, only those atoms which pass through the most intense part of the laser beam will contribute significantly to the measurement.

During a measurement it is often necessary to readjust the Fabry-Pérot instruments. This is done in the following way. An experimental run is interrupted when the count rate is decreased by 20%. The electronic stabilization unit of the Fabry-Pérot devices then optimizes the finesse and mean mirror spacing. About every hour this procedure is repeated manually since the electronics was not able to optimize the finesse perfectly. For experiments on resonance the laser frequency is readjusted at the same time. The frequency drift of the laser is about 130 MHz per hour. After readjustment the count rates of the photomultipliers are reproduced to within about 2%.

The full width at half maximum (FWHM) ($=2\gamma$) of the RC-150 is 0.55 GHz and that of the RC-110 is 0.82 GHz. Hence for $\Omega=4.3$ GHz and $\Delta=0$ the transmission factor for the other triplet components is 5×10^{-3} for the RC-150 and 9×10^{-3} for the RC-110.

In Figs. 6–14 the solid line is a least-squares fit of (42) to the data points. In all fits the Einstein coefficient A was fixed at 1.2×10^{8} s^{-1}. The Rabi frequency Ω and the

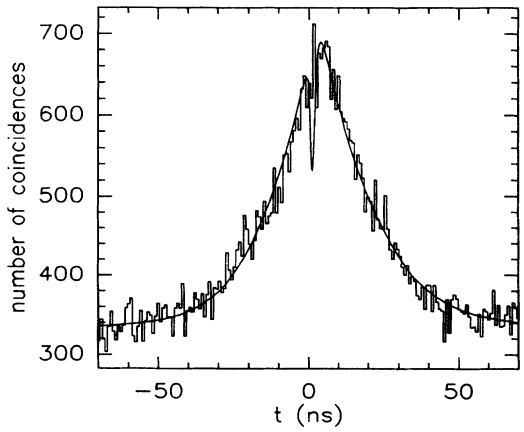

FIG. 6. The correlation function $\bar{I}_2(TF;t)\xi(t)$; $\Delta=0.0(3)$ GHz and $\Omega=4.3(2)$ GHz. The solid line represents a least-squares fit of (42) to the data points.

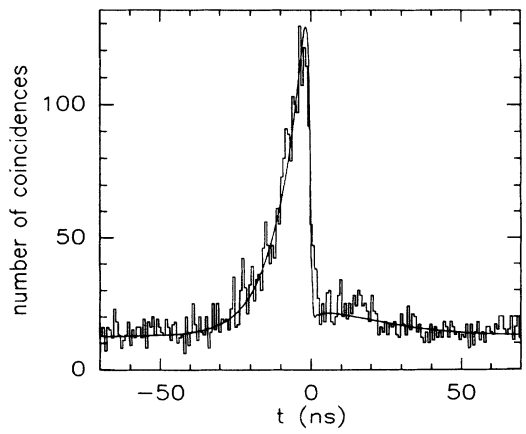

FIG. 8. The same as Fig. 6. $\Delta=-3.1(5)$ GHz and $\Omega=3.8(2)$ GHz.

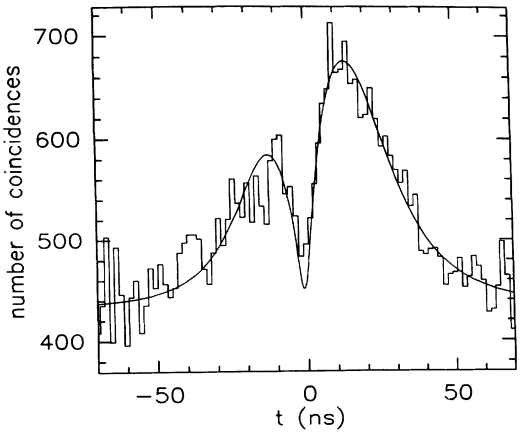

FIG. 9. The correlation function $\bar{I}_2(FF;t)\xi(t)$; $\Delta=0.0(3)$ GHz and $\Omega=5.0(3)$ GHz.

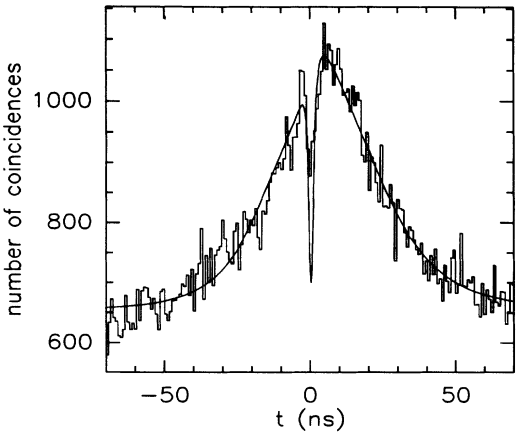

FIG. 12. The correlation function $\bar{I}_2(FR;t)\xi(t)$; $\Delta=0.0(3)$ GHz and $\Omega=4.0(5)$ GHz.

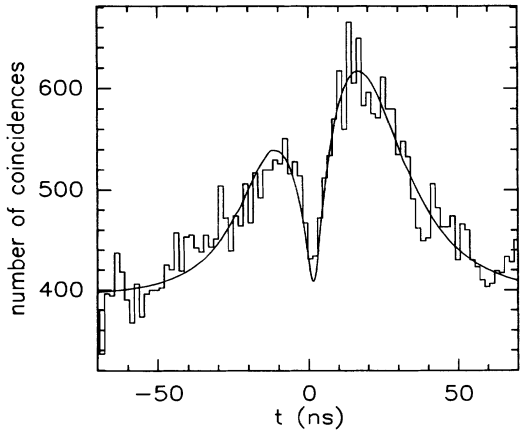

FIG. 10. The correlation function $\bar{I}_2(TT;t)\xi(t)$; $\Delta=0.0(3)$ GHz and $\Omega=4.2(3)$ GHz.

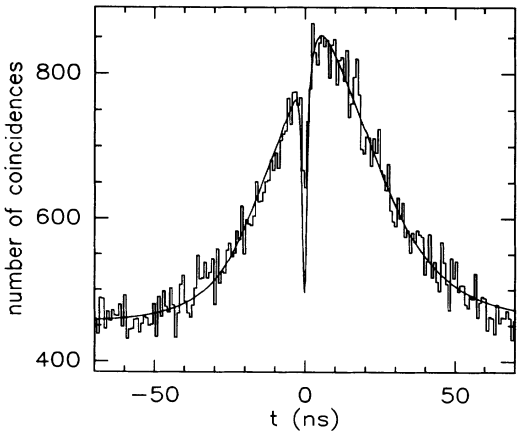

FIG. 13. The correlation function $\bar{I}_2(TR;t)\xi(t)$; $\Delta=0.0(3)$ GHz and $\Omega=4.0(5)$ GHz.

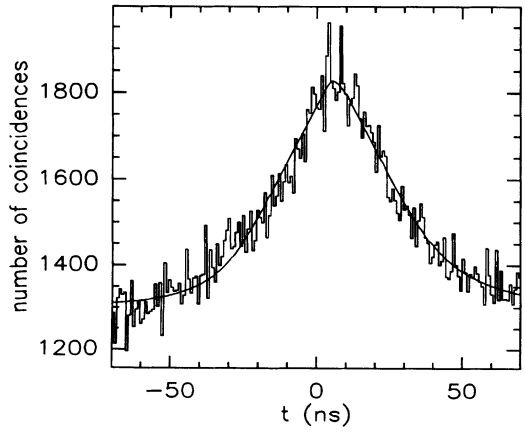

FIG. 11. The correlation function $\bar{I}_2(RR;t)\xi(t)$; $\Delta=0.0(3)$ GHz and $\Omega=4.0(5)$ GHz.

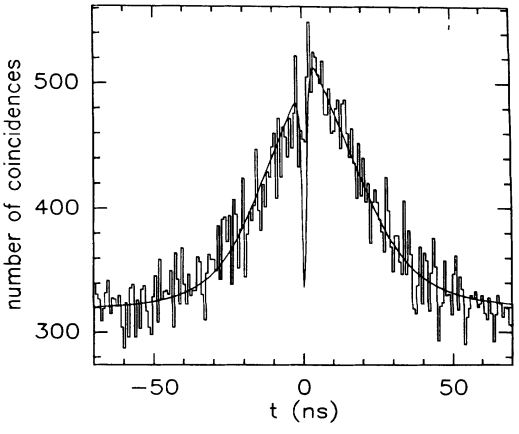

FIG. 14. The correlation function $\bar{I}_2(FR;t)\xi(t)$; $\Delta=-2.0(3)$ GHz and $\Omega=4.6(3)$ GHz.

detuning Δ are determined from measurements on the fluorescence triplet.

For $\Delta<0$ the F photons originate from the sideband at the higher-frequency side of the R line and T photons from the opposite sideband. In this article we adopt the convention that this is also the case on resonance, although on resonance the assignment of the sidebands as F line or T line is arbitrary, as mentioned before.

A. FT and TF experiments

Figures 6, 7, and 8 show the plots of three spectra which were recorded with the start of the TAC triggered by a photon from the higher-frequency sideband and the stop triggered by a photon from the lower-frequency sideband. The measuring times for the three spectra shown here were 5, 4.2, and 1.9 h, respectively. The average number of atoms in the interaction volume varied between 1.5 and 2.

The spectra are strongly influenced by the transit function $\xi(t)$. In our experimental circumstances it is necessary to choose the length l rather short. The combined requirements that $\Omega \gg A$ and that the laser intensity is fairly homogeneous over the interaction volume led us to the choice $l \approx 20$ μm. This implies that $\tau_0 \approx 55$ ns for an oven temperature of 1100 K. Note that this is much larger than Ω^{-1} (≈ 0.3 ns), so that the assumption of a steady state, as was made in the theory of Chaps. II and III, is justified. The transit function has yet another effect on the measured spectra. For $\Delta=0$ the measured correlation function is asymmetric ($q=0.85$). This is caused by an imperfection in the alignment of the detection optics: the two observation volumes do not coincide perfectly. This asymmetry has also been taken into account in the other experiments.

In the two spectra for $\Delta \neq 0$ the measured correlation function shows a maximum of coincidences for $t<0$. This asymmetry becomes more pronounced if $|\Delta|$ is increased.

In Fig. 7 deviations from the fit function are visible near $+20$ and -20 ns. The observed bumps are caused by reflections on the Fabry-Pérot devices. A photon from the T line will be reflected by the Fabry-Pérot device which is tuned to the F peak. This reflected photon is seen by the interferometer which is tuned to the T line. Hence this delayed photon can cause a true coincidence. However, the measured correlation function will be shifted over $2L/c$, with L the distance between interaction volume and interferometer, and c is the speed of light. The distance between the Fabry-Pérot interferometers and the vacuum apparatus is about 3 m, which is consistent with the measured time delay of about 20 ns.

Equations (40a) and (40b) predict a dip for $\Delta=0$ and $t \lesssim \gamma^{-1}$. However, we did not observe such a dip. This is probably due to the finite time resolution of the detection electronics (3 ns).

B. FF and TT experiments

In Figs. 9 and 10 the spectra of an FF and a TT measurement on resonance are given, respectively. In the FF experiment both Fabry-Pérot devices are tuned to the higher-frequency sideband and in the TT experiment both are tuned to the lower-frequency sideband. As expected from (28) and (42), the measured correlation function drops to the background level of accidental coincidences as t approaches zero. In our experimental circumstances these measurements are the most difficult ones since the measured correlation function is very noisy: the maximum of this function is determined by the maximum of the product of the correlation function and the transit function. This maximum is smaller than one. This implies that the average number of atoms in the interaction region should be smaller than one. In the two spectra shown here the average number of atoms in the interaction volume was 0.86 (measuring time 10 h).

C. RR experiments

According to (36) the correlation function in this case is equal to one for all t. Therefore the measured correlation function shown in Fig. 11 only reflects the behavior of the transit function. We also performed an experiment with a small detuning (not shown here). The measured correlation function did not appear to be affected by a change in the detuning, which is in accordance with the theory.

D. TR and FR experiments

Figures 12, 13, and 14 show the results of measurements on the correlation functions in which one R photon is involved. According to (38) and (39) a correlation function is expected which equals one for $t \gg \gamma^{-1}$ and zero for $t=0$. The two spectra for $\Delta=0$ (Figs. 12 and 13) show a decrease in the number of coincidences near $t=0$. However, the observed dip near $t=0$ does not drop all the way to the background level of accidental coincidences. This is due to the finite time resolution of the detection electronics (3 ns).

We also did some TR and FR experiments off resonance. In Fig. 14 the results are shown of an FR experiment where $\Delta/\Omega \approx 0.5$. In these cases the interference effect is less pronounced. Probably the interference dip is obscured by unwanted RR correlations.

VI. CONCLUSIONS

We have extended the theoretical description of spectrally resolved photon correlations between the components of the fluorescence triplet. The extension lies in the fact that we allow the time difference between two successive photon detections to be smaller than the inverse bandwidth of the interferometers. The correlation function for a photon in a sideband and a photon from the central Rayleigh line is found to display a dip with a width of the order of the inverse interferometer bandwidth. The resulting antibunching behavior can be explained in the dressed-atom picture as a destructive interference between the time orderings of emission of the two photons. The destructive interference is possible due to the uncertainty in the emission times for an observed time of detection. This uncertainty arises in the inter-

ferometer, which illustrates that the correlation function for spectrally resolved photons is a property of the combined system of the fluorescent atom and the interferometers. A similar dip is predicted for the correlation function between two photons from opposite sidebands.

We have measured the time correlations between spectrally resolved photons resulting from the fluorescence triplet of the $^1S_0 \leftrightarrow {}^1P_1$ transition of natural barium. Measurements have been performed on all six combinations of photons from the components of the fluorescence triplet. In all the experiments the tuning of the laser was close to or on resonance. The predictions based on existing theory are confirmed for the case where the time difference between the detected photons is larger than the inverse-frequency width of the interferometer. The short-time behavior of the correlation functions, sketched in this paper, is also confirmed in most experiments. However, in some cases the theoretical predictions near $t=0$ are obscured by the time resolution of the electronics and unwanted RR correlations.

*Present address: Max-Planck-Institut für Quantenoptik, D-8046 Garching, Germany.

†Present address: Huygens Laboratorium, Rijksuniversiteit Leiden, Postbus 9504, 2300 RA Leiden, The Netherlands.

[1] M. Newstein, Phys. Rev. **167**, 89 (1968).

[2] B. R. Mollow, Phys. Rev. **178**, 1969 (1969).

[3] F. Y. Wu, R. E. Grove, and S. Ezekiel, Phys. Rev. Lett. **35**, 1426 (1975); W. Hartig, W. Rasmussen, R. Schieder, and H. Walther, Z. Phys. A **278**, 205 (1976); J. L. Carlsten and A. Szöke, Phys. Rev. Lett. **36**, 667 (1976); R. E. Grove, F. Y. Wu, and S. Ezekiel, Phys. Rev. A **15**, 227 (1977); S. Cavalieri, R. Buffa, M. Matera, and M. Mazzoni, J. Phys. B **20**, 5363 (1987); J. E. Golub and T. W. Mossberg, Phys. Rev. Lett. **59**, 2149 (1987).

[4] C. Cohen-Tannoudji and S. Reynaud, Philos. Trans. R. Soc. London Ser. A **293**, 223 (1979).

[5] J. H. Eberly and K. Wódkiewicz, J. Opt. Soc. Am. **67**, 1252 (1977).

[6] S. Reynaud, Ann. Phys. (Paris) **8**, 315 (1983).

[7] H. F. Arnoldus and G. Nienhuis, J. Phys. B **17**, 963 (1984).

[8] A. Aspect, G. Roger, S. Reynaud, J. Dalibard, and C. Cohen-Tannoudji, Phys. Rev. Lett. **45**, 617 (1980).

[9] R. J. Glauber, *Quantum Optics and Electronics,* edited by C. DeWitt, A. Blandin, and C. Cohen-Tannoudji (Gordon and Beach, New York, 1965).

[10] H. J. Kimble and L. Mandel, Phys. Rev. A **13**, 2123 (1976).

[11] G. S. Agarwal, *Quantum Statistical Theories of Spontaneous Emission and their Relation to Other Approaches,* Springer Tracts in Modern Physics Vol. 70 (Springer, Berlin, 1974).

[12] M. Dagenais and L. Mandel, Phys. Rev. A **18**, 2217 (1978).

[13] R. Short and L. Mandel, Phys. Rev. Lett. **51**, 384 (1983).

[14] L. Knöll, W. Vogel, and D.-G. Welsh, J. Opt. Soc. Am. B **3**, 1305 (1986).

[15] J. D. Cresser, J. Phys. B **20**, 4915 (1987).

[16] G. Nienhuis, J. Phys. B **14**, 3117 (1981).

[17] C. Cohen-Tannoudji and S. Reynaud, J. Phys. B **10**, 345 (1977).

[18] P. A. Apanasevich and S. Ja. Kilin, J. Phys. B **12**, L83 (1979).

[19] H. J. Kimble, M. Dagenais, and L. Mandel, Phys. Rev. Lett. **39**, 691 (1977).

[20] D. A. Lewis, J. Kumar, M. A. Finn, and G. W. Greenless, Phys. Rev. A **35**, 131 (1987).

[21] S. Niggli and M. C. E. Huber, Phys. Rev. A **35**, 2908 (1987).

[22] F. Spieweck, Appl. Phys. B **29**, 99 (1982).

[23] H. J. Kimble, M. Dagenais, and L. Mandel, Phys. Rev. A **18**, 201 (1978).